On the destabilizing nature of capital gains taxes

On the destabilizing nature of capital gains taxes[*,**]

Roberto Dieci[a], Laura Gardini[b], Frank Westerhoff[c,***]

[a] Department of Mathematics and School of Economics and Management, University of Bologna, Bologna, Italy

[b] Department of Economics, Society and Politics, University of Urbino Carlo Bo, Italy

[c] Department of Economics, University of Bamberg, Germany

Abstract

Policymakers around the world impose some form of capital gains taxes to foster the stability of financial markets. Unfortunately, there is no clarity on the effects of capital gains taxes. Based on a stylized behavioral asset-pricing model highlighting the trading activity of extrapolating speculators, we show that policymakers may involuntary destabilize financial markets by imposing capital gains taxes. Most importantly, we find that the imposition of capital gains taxes may trigger endogenous cyclical asset price dynamics occurring around inflated price levels. A number of robustness checks in which we allow for interactions between speculators who use extrapolative and regressive expectation rules confirm our main results.

Keywords

Asset price dynamics; capital gains taxes; expectation formation; systematic mispricing and excess volatility; piecewise linear maps.

JEL classification

G12; G18; G41.

---

* Declarations of interest: none.

** We thank two anonymous referees for their valuable and constructive feedback on our paper.

*** Contact: Frank Westerhoff, University of Bamberg, Department of Economics, Feldkirchenstrasse 21, 96045 Bamberg, Germany. Email: frank.westerhoff@uni-bamberg.de.

1 Introduction

Littlewood and Elliffe (2017) report that almost all countries around the world impose some form of capital gains tax. By taxing capital gains, policymakers seek to foster the stability of financial markets by taming speculators' trading activity. Unfortunately, there is no clarity on the effects of capital gains taxes. According to the capitalization hypothesis, capital gains taxes reduce asset prices because speculators demand a lower price when buying assets on which they will have to pay capital gains taxes some time in the future. In contrast, the lock-in hypothesis states that capital gains taxes increase asset prices because speculators require higher prices to sell assets on which they must pay capital gains taxes. See Klein (1999), Poterba and Weisbenner (2001), Ayers et al. (2003) and Dai et al. (2008) for a discussion of the equilibrium effects of capital gains taxes surrounding these opposing demand and supply arguments. We are particularly interested in the dynamic consequences of capital gains taxes. Based on a stylized behavioral asset-pricing model, we show that capital gains taxes may endanger the stability of financial markets. Most importantly, we find that policymakers may create excess volatility and systematic mispricing around inflated price levels by imposing capital gains taxes.

To study the effects of capital gains taxes, we adapt the seminal asset-pricing model by Brock and Hommes (1998), assuming that speculators can invest in a safe asset and in a risky asset. Moreover, speculators are myopic mean-variance maximizers who are interested in their end-of-period wealth and rely on an extrapolative expectation rule to predict the price of the risky asset. In the absence of capital gains taxes, the price of the risky asset is due to the iteration of a two-dimensional linear map, and converges towards its fundamental value, given by the discounted value of expected future risk-adjusted dividend payments, provided that certain stability conditions are met. However, speculators' optimal demand for the risky asset is state-dependent in the presence of capital gains taxes. In particular, speculators' demand for the risky asset depends on the tax rate imposed on capital gains when they expect an increase in the price of the risky asset. Otherwise, they do not expect to make capital gains, and their demand for the risky asset is independent of capital gains taxes. Accordingly, a two-dimensional piecewise linear map with two branches determines the price of the risky asset when policymakers

impose capital gains taxes: a tax branch, relevant in upward trending markets, and a non-tax branch, relevant in downward trending markets.

To be able to understand the destabilizing nature of capital gains taxes, it is crucial to realize that each of the two branches of the model's map is associated with a different fixed point – a real fixed point and a virtual fixed point. When speculators expect a downturn, their demand for the risky asset is independent of capital gains taxes. The real fixed point price of the risky asset then corresponds to the discounted value of expected future risk-adjusted dividend payments – as in a world without capital gains taxes. When speculators expect an upturn, however, their demand for the risky asset depends on capital gains taxes, and the price of the risky asset possesses a further virtual fixed point that is located above the real (fundamental) fixed point price of the risky asset. The difference between the two fixed points depends on the state-dependent risk premium of the risky asset. In a nutshell, the economic intuition for this result may be grasped as follows. Note first that capital gains taxes reduce fluctuations in speculators' wealth, an outcome that diminishes the risk associated with holding the risky asset. Since this makes – ceteris paribus – the risky asset more attractive, speculators' increased demand pressure elevates the virtual fixed point price of the risky asset above its real fixed point price. The reason why the second fixed point is a virtual fixed point is that speculators do not pay capital gains taxes when the risky asset market is at rest.[1]

Capital gains taxes may endanger the stability of financial markets in several ways. In the following, we preview one of our most intriguing results by outlining how the imposition of capital gains taxes may create endogenous cyclical asset price dynamics, in spite of the fact that the model's parameters imply that both fixed points are stable foci. In the absence of capital gains taxes, this furthermore implies that such a model parameterization would yield an oscillatory convergence towards the risky asset's fundamental value. We also observe such dynamics when policymakers impose capital gains taxes, albeit – and this is crucial – only as long as the price of the risky asset decreases. However, the oscillatory nature of the risky asset's price dynamics implies that its price will fall below its real fixed

[1] Technically speaking, a virtual fixed point of a branch of a piecewise-defined map is a fixed point that exists outside the domain for which the branch is defined. Nevertheless, a virtual fixed point may have a significant impact on the overall dynamics of the model.

point during the adjustment phase, and then start to reverse its direction. Consequently, a regime change occurs. Since speculators then start to expect a price recovery, the virtual fixed point begins to attract the price of the risky asset. Since the virtual fixed point is a stable focus, we observe overshooting during the adjustment phase and, again, a reversal of the risky asset's price direction, the triggering point where the next regime change takes place and where the real fixed point price of the risky asset becomes the relevant attractor for its dynamics again. As a result, permanent endogenous asset price fluctuations around an elevated price level are set in motion. We remark that empirical studies by Blouin et al. (2003), Jin (2006), George and Hwang (2007) and Jacob (2018) also report that capital gains taxes tend to inflate asset prices. Moreover, the transition from fixed-point dynamics to cyclical dynamics may be dramatic. The moment when the aforementioned cycles emerge, they may already possess a significant amplitude, i.e. we observe a sharp jump in volatility and mispricing. A number of robustness checks in which we allow for interactions between speculators who rely on extrapolative and regressive expectation rules confirm our main results.

Our work is related to a line of literature that regards financial markets as expectation-driven feedback systems. See Zeeman (1974), Beja and Goldman (1998), Day and Huang (1990), Lux (1995) and Brock and Hommes (1998) for pioneering contributions, and Chiarella et al. (2009), Hommes (2013), Dieci and He (2018) and He et al. (2019) for surveys. To gain deeper analytical insights into the functioning of such systems, a part of this flourishing literature stream started to consider simplified financial market models that – technically speaking – take the form of piecewise linear maps. See, for instance, the seminal work by Huang and Day (1993) and the follow-up papers by Huang et al. (2010, 2012) and Tramontana et al. (2010, 2013). Note that these contributions operate at the intersection of economics and mathematical sciences, offering new mathematical results that facilitate our understanding of the behavior of piecewise maps. See Avrutin et al. (2019) for an overview. The same is true for our paper. From a mathematical perspective, our paper advances the analytical and numerical treatment of two-dimensional piecewise linear maps that are characterized by change-dependent branches. Finally, we note that expectation-driven financial market models have proven quite valuable in evaluating and assessing the effectiveness of regulatory policies in the recent past. See Westerhoff

(2008) and Westerhoff and Franke (2018) for reviews. In this respect, we note that the effects of capital gains taxes described in our paper are, at least in a broader sense, reminiscent of those of short-selling constraints found in Anufriev and Tuinstra (2013) and Dercole and Radi (2020). Short-selling constraints may imply state-dependent restrictions on speculators' demand schedules, too, resulting in endogenous asset price fluctuations occurring around elevated price levels.

We continue as follows. In Section 2, we introduce a stylized behavioral asset-pricing model in which extrapolating speculators may be subject to capital gains taxes. In Section 3, we present our main results. In Section 4, we conduct a number of robustness checks. In particular, we consider that speculators may switch between extrapolative and regressive expectation rules. In Section 5, we conclude our paper.

2 A stylized behavioral asset-pricing model

We adapt the seminal asset-pricing framework by Brock and Hommes (1998) to study a number of intriguing effects of capital gains taxes. To make our arguments on the destabilizing nature of capital gains taxes as stark as possible, we simplify their framework by assuming that speculators rely on an extrapolative expectation rule to predict the price of the risky asset.[2] Moreover, we assume that speculators address their rather complicated wealth allocation problem by considering only two possible future regimes: a capital gains tax regime, relevant when they expect the price of the risky asset to increase, and a regime with no capital gains tax, relevant when they expect the price of the risky asset to decrease. Finally, we assume that dividend payments from the risky asset create no additional risk for speculators, i.e. its random dividend component has already been realized for the period in which they make their investment decisions. Hence, the only risk speculators face stems from the uncertainty surrounding the price dynamics of the risky asset.

Let us turn to the details of our model. Speculators can invest in a safe asset, paying the risk-free interest rate r, and in a risky asset, paying dividend D_t. Dividend payments from

[2] Note that Glaeser and Nathanson (2017) make a similar simplifying assumption to be able to study the dynamics of speculative housing markets.

the risky asset are represented by an IID dividend process with a constant mean, i.e. $D_t = \overline{D} + \delta_t$, with $\delta_t \sim N(0, \sigma_\delta^2)$. The safe asset is perfectly elastically supplied, an assumption that fixes its price. The price of the risky asset changes with respect to speculators' trading activity, which we model in the following. Let P_t be the price of the risky asset at time t; Z_t^i speculator i's demand for the risky asset, measured in terms of the (positive) number of shares acquired in period t; and $0 \leq \tau < 1$ the tax rate imposed by policymakers on speculator i's capital gains. Speculator i's wealth in period $t+1$ then reads

$$W_{t+1}^i = \begin{cases} (1+r)W_t^i + Z_t^i(P_{t+1} + D_t - (1+r)P_t) - \tau(P_{t+1} - P_t)Z_t^i & if\ P_{t+1} - P_t > 0 \\ (1+r)W_t^i + Z_t^i(P_{t+1} + D_t - (1+r)P_t) & if\ P_{t+1} - P_t \leq 0 \end{cases}, \quad (1)$$

where the term $\tau(P_{t+1} - P_t)Z_t^i$ reflects his capital gains tax payments, due if the price of the risky asset increases between periods t and $t+1$. Note that speculator i regards P_{t+1}, and consequently W_{t+1}, as random variables. Brock and Hommes (1998) assume that speculator i is a myopic mean-variance maximizer who derives his demand for the risky asset from solving the optimization problem

$$max_{Z_t^i} \left\{ E_t^i\left[W_{t+1}^i\right] - \frac{\lambda}{2} V_t^i\left[W_{t+1}^i\right] \right\}. \quad (2)$$

Here, $E_t^i\left[W_{t+1}^i\right]$ and $V_t^i\left[W_{t+1}^i\right]$ denote speculator i's subjective beliefs about the conditional expectation and conditional variance of his wealth, respectively, and λ is a positive risk aversion parameter.

Obviously, policymakers' (nonlinear) capital gains taxation turns speculator i's maximization problem into an intricate task.[3] We address this issue via the following behavioral argument. Let us first recall that experimental evidence supports the notion of bounded rationality. As made clear by Simon (1955), Tversky and Kahneman (1974) and Hirshleifer (2001), human agents do not possess perfect knowledge, nor do they have the computational capacity to derive optimal actions. Instead, human agents rely on a limited number of heuristic principles, which help them to cope with complex decision tasks. Since

[3] Unlike in the Brock and Hommes (1998) framework, in our model both $E_t^i[W_{t+1}^i]$ and $V_t^i\left[W_{t+1}^i\right]$ are nonlinear functions of the hypothetical price P_t. Even if we assume that P_{t+1} is conditionally normally distributed in agents' beliefs, W_{t+1}^i has a complicated non-Gaussian distribution function (it is related to a truncated normal distribution, in which the truncation point P_t is itself a parameter that varies in speculators' demand schedule), implying that $E_t^i\left[W_{t+1}^i\right]$ and $V_t^i\left[W_{t+1}^i\right]$ do not only depend on the first and second moment of P_{t+1}, but on its whole distribution.

people share similar heuristics, their aggregated impact is significant. Representativeness is one of the most salient heuristics. According to Tversky and Kahneman (1974), human agents following the representativeness heuristic classify things into discrete categories based on similarity considerations. Importantly, human agents typically use few observations to identify similarity. Due to the complexity of speculators' optimization problem, we assume that speculators follow the representativeness heuristic. Accordingly, speculators simplify their decision problem by considering two polar opposite regimes: a capital gains tax regime, relevant when they expect the price of the risky asset to increase, and a regime with no capital gains tax, relevant when they expect the price of the risky asset to decrease.[4]

More precisely, speculator i forms his beliefs about the future price of the risky asset $E_t^i[P_{t+1}]$ based on information available up to period $t-1$, and sets his beliefs about the variance of the price of the risky asset equal to $V_t^i[P_{t+1}] = \sigma^2$. Furthermore, speculator i uses past price information as an indicator of whether the capital gains tax regime or the regime with no capital gains tax will unfold. If $E_t^i[P_{t+1}] > P_{t-1}$, speculator i regards the regime with upward price adjustments and capital gain tax payments as the relevant future regime, and maximizes (2) subject to the upper branch of (1). If $E_t^i[P_{t+1}] < P_{t-1}$, speculator i regards the regime with downward price adjustments and no capital gains tax payments as the relevant regime, and maximizes (2) subject to the lower branch of (1). In the former case, speculator i's demand for the risky asset is given by $Z_t^i = \frac{(1-\tau)E_t^i[P_{t+1}]+D_t-(1+r-\tau)P_t}{(1-\tau)^2\lambda V_t^i[P_{t+1}]}$, and in the latter case by $Z_t^i = \frac{E_t^i[P_{t+1}]+D_t-(1+r)P_t}{\lambda V_t^i[P_{t+1}]}$.[5] Hence, speculator i's demand for the risky asset results in

$$Z_t^i = \begin{cases} \frac{(1-\tau)E_t^i[P_{t+1}]+D_t-(1+r-\tau)P_t}{(1-\tau)^2\lambda\sigma^2} & if\ E_t^i[P_{t+1}] - P_{t-1} > 0 \\ \frac{E_t^i[P_{t+1}]+D_t-(1+r)P_t}{\lambda\sigma^2} & if\ E_t^i[P_{t+1}] - P_{t-1} \leq 0 \end{cases}. \tag{3}$$

[4] Clearly, the two regimes are two different categories, and price trends are used to identify them.

[5] Note that $E_t^i[W_{t+1}^i] = (1+r)W_t^i + Z_t^i(E_t^i[P_{t+1}] + D_t - (1+r)P_t) - \tau(E_t^i[P_{t+1}] - P_t)Z_t^i$ and $V_t^i[W_{t+1}^i] = (1-\tau)^2 V_t^i[P_{t+1}](Z_t^i)^2$ in the capital gains tax regime, implying that speculator i's first-order condition reads $(1-\tau)E_t^i[P_{t+1}] + D_t - (1+r-\tau)P_t - \lambda(1-\tau)^2 V_t^i[P_{t+1}]Z_t^i = 0$. Moreover, capital gains taxes linearly decrease $E_t^i[W_{t+1}^i]$, while they quadratically decrease $V_t^i[W_{t+1}^i]$.

Since speculator i uses the extrapolative expectation rule

$$E_t^i[P_{t+1}] = P_{t-1} + \chi(P_{t-1} - P_{t-2}), \tag{4}$$

with χ as a positive extrapolation parameter, we can eventually express his demand for the risky asset by

$$Z_t^i = \begin{cases} \frac{(1-\tau)(P_{t-1}+\chi(P_{t-1}-P_{t-2}))+D_t-(1+r-\tau)P_t}{(1-\tau)^2\lambda\sigma^2} & if\ P_{t-1} - P_{t-2} > 0 \\ \frac{P_{t-1}+\chi(P_{t-1}-P_{t-2})+D_t-(1+r)P_t}{\lambda\sigma^2} & if\ P_{t-1} - P_{t-2} \leq 0 \end{cases}. \tag{5}$$

Clearly, speculator i selects the upper or the lower branch of his demand schedule, (5), depending on whether the last observable price change was positive or negative.

Assuming that there are N speculators in total, speculators' aggregate demand for the risky asset amounts to

$$Z_t = \sum_{i=1}^{N} Z_t^i. \tag{6}$$

Market equilibrium requires that the demand for the risky asset equals its supply. Thus,

$$Z_t = S_t, \tag{7}$$

where the supply of the risky asset, i.e. the number of shares offered by firms, is constant and set at

$$S_t = \hat{S} = N\bar{S}. \tag{8}$$

For notational convenience, we introduce $\bar{S}$ as the (average) number of shares of the risky asset available per speculator. Due to our assumption that speculators are homogenous, it is immediately apparent that the market-clearing price generated by equilibrium condition (7) will ensure that each speculator holds the same (positive) number of shares of the risky asset at each time step, namely $Z_t^i = \bar{S} > 0$. Hence, speculators do not engage in short selling in our model, as implicitly assumed by our setup of capital gains taxes in their wealth equations (1).

3 Main insights

3.1 Preliminary observations

Since we are interested in the properties of the model's deterministic skeleton, we abstract in the following from dividend shocks, i.e. we set $D_t = \overline{D}$. Combining (5) to (8) and introducing the auxiliary variable $X_t = P_{t-1}$ then reveals that our model may be represented by the two-dimensional piecewise linear map

$$C:\begin{cases} P' = \begin{cases} \frac{(1-\tau)(P+\chi(P-X))+\bar{D}-(1-\tau)^2\lambda\sigma^2\bar{S}}{1+r-\tau} & if\ P > X \\ \frac{P+\chi(P-X)+\bar{D}-\lambda\sigma^2\bar{S}}{1+r} & if\ P \leq X \end{cases} \\ X' = P \end{cases}, \tag{9}$$

where the prime symbol denotes the unit time advancement operator. For $\tau = 0$, the model's complete map C simplifies to the reduced map

$$R:\begin{cases} P' = \frac{P+\chi(P-X)+\bar{D}-\lambda\sigma^2\bar{S}}{1+r} \\ X' = P \end{cases}. \tag{10}$$

To facilitate the analysis, let us subdivide the complete map of the model into two sub-maps. For $P \leq X$, we obtain the sub-map

$$T_u:\begin{cases} P' = \frac{P+\chi(P-X)+\bar{D}-\lambda\sigma^2\bar{S}}{1+r} \\ X' = P \end{cases}, \tag{11}$$

which is relevant above and on the diagonal $X = P$ in the (P, X)-phase plane. For $P > X$, we obtain the sub-map

$$T_l:\begin{cases} P' = \frac{(1-\tau)(P+\chi(P-X))+\bar{D}-(1-\tau)^2\lambda\sigma^2\bar{S}}{1+r-\tau} \\ X' = P \end{cases}, \tag{12}$$

which is relevant below the diagonal $X = P$ in the (P, X)-phase plane. Note that sub-map T_u is identical to the model's reduced map R, except, of course, with respect to their domains of definition.

Let us first study sub-map T_u. Straightforward computations reveal that this sup-map has a real fixed point, given by

$$F \coloneqq \bar{P} = \bar{X} = \frac{\bar{D}-\lambda\sigma^2\bar{S}}{r}. \tag{13}$$

The corresponding Jacobian matrix reads

$$J_u = \begin{bmatrix} \frac{1+\chi}{1+r} & -\frac{\chi}{1+r} \\ 1 & 0 \end{bmatrix}, \tag{14}$$

with $Tr_u := \frac{1+\chi}{1+r}$ and $Det_u := \frac{\chi}{1+r}$. As is well known, the stability of a fixed point of a two-dimensional linear map depends on the set of inequalities (i) $1 + Tr + Det > 0$, (ii) $1 - Tr + Det > 0$ and (iii) $1 - Det > 0$.[6] The first two conditions are always satisfied, while the

[6] See Medio and Lines (2001), Gandolfo (2009) and Puu (2013) for excellent introductions to the field of nonlinear (economic) dynamics.

third one requires that

$$\chi < 1 + r. \tag{15}$$

Assume that (15) holds. The real fixed point F is then a stable focus for $Tr^2 < 4Det$, leading to

$$\frac{(1+\chi)^2}{4\chi} < 1 + r, \tag{16}$$

or, equivalently, $(1-\chi)^2 < 4\chi r$. If (15) holds and if the inequality sign in (16) is reversed or binding, the real fixed point F is a stable node. In this case, the real eigenvalues associated with the stable node are always positive and can be expressed by

$$\lambda_{\pm} = \frac{1}{2(1+r)}[(1+\chi) \pm \sqrt{(1-\chi)^2 - 4r\chi}], \tag{17}$$

with eigenvectors that are straight lines $V_{\pm}$ running through the coordinates of the real fixed point F with slopes

$$s_{\pm} = \frac{2(1+r)}{(1+\chi) \pm \sqrt{(1-\chi)^2 - 4r\chi}}. \tag{18}$$

In the (P, X)-phase plane, the straight lines have equations

$$X = F + s_{\pm}(P - F), \tag{19}$$

with $s_+ < s_-$. Recall that a stable node with positive eigenvalues is monotonically approached via the straight lines defined by its eigenvectors.

Let us now turn to sub-map T_l, which possesses the fixed point

$$P^v := \bar{P} = \bar{X} = \frac{\bar{D} - (1-\tau)^2 \lambda \sigma^2 \bar{S}}{r}. \tag{20}$$

We call (20) a virtual fixed point since it is not defined for the model's complete map C. Since the Jacobian matrix of sub-map T_l reads

$$J_l = \begin{bmatrix} \frac{(1-\tau)(1+\chi)}{1+r-\tau} & -\frac{(1-\tau)\chi}{1+r-\tau} \\ 1 & 0 \end{bmatrix}, \tag{21}$$

with $Tr_l := \frac{(1-\tau)(1+\chi)}{1+r-\tau}$ and $Det_l := \frac{(1-\tau)\chi}{1+r-\tau}$, we can conclude that stability conditions $1 + Tr + Det > 0$ and $1 - Tr + Det > 0$ always hold. However, it follows from the remaining stability condition $1 - Det > 0$ that the virtual fixed point is attracting in the case of

$$\chi < \frac{1+r-\tau}{1-\tau}. \tag{22}$$

Assume that (22) holds. It then follows from $Tr^2 < 4Det$ that the virtual fixed point is a stable focus if

$\frac{(1+\chi)^2}{4\chi} < \frac{1+r-\tau}{1-\tau}$, (23)

being equivalent to $(1-\tau)(1-\chi)^2 < 4\chi r$, or a stable node, provided that the inequality sign in (23) is reversed or binding. Once again, the real eigenvalues associated with the stable node are always positive and can be written as

$\lambda_{\pm} = \frac{1}{2(1+r-\tau)}[(1-\tau)(1+\chi) \pm \sqrt{(1-\tau)^2(1-\chi)^2 - 4r\chi(1-\tau)}]$, (24)

with eigenvectors that are straight lines $VP_{\pm}$ running through the coordinates of virtual fixed point P^v with slopes

$sp_{\pm} = \frac{2(1+r-\tau)}{(1-\tau)(1+\chi) \pm \sqrt{(1-\tau)^2(1-\chi)^2 - 4r\chi(1-\tau)}}$. (25)

In the (P, X)-phase plane, the straight lines $VP_{\pm}$ have equations

$X = P^v + sp_{\pm}(P - P^v)$, (26)

with $sp_+ < sp_-$, determining the monotonic adjustment path towards the stable node.

A few comments are in order:

- For $\tau = 0$, i.e. in the absence of capital gains taxes, the price of the risky asset is driven by the reduced map (10). It possess a unique fundamental fixed point, given by $F = \frac{\bar{D} - \lambda\sigma^2\bar{S}}{r}$, at which the price of the risky asset is equal to the discounted value of expected future risk-adjusted dividend payments, referred to as the fundamental value of the risky asset. Moreover, this fixed point is globally stable, provided that $\chi < 1 + r$. Accordingly, the risky asset market may become unstable if speculators extrapolate past price changes too strongly, although a reduction in the interest rate may also compromise its stability. Finally, if the fundamental fixed point F is stable, then it is either a stable focus (with complex eigenvalues) or a stable node (with positive eigenvalues), depending on whether $\frac{(1+\chi)^2}{4\chi}$ is smaller than $1 + r$ or not. In the former case, the price of the risky asset approaches its fundamental value in the form of cycles with decreasing amplitude. In the latter case, the price of the risky asset monotonically approaches its fundamental value.
- For $\tau > 0$, i.e. in the presence of capital gains taxes, the price of the risky asset is jointly driven by sub-maps (11) and (12); it therefore possesses a real (fundamental) fixed point and an additional virtual fixed point. Note that the virtual fixed point implies a higher

level of the risky asset's price than the real fixed point. The economic rationale for this result is as follows. First, we can interpret $\Delta = \lambda\sigma^2\bar{S}$ as the pre-tax risk premium of the risky asset. Comparing $F = \frac{\bar{D}-\Delta}{r}$ and $P^v = \frac{\bar{D}-(1-\tau)^2\Delta}{r}$ immediately reveals that capital gains taxes reduce the actual (effective) risk premium of the risky asset, driving up its price.[7] To say it in more detail, speculators' demand for the risky asset at a hypothetical fixed point P^*, given by $Z^* = \frac{\bar{D}-rP^*}{(1-\tau)^2\lambda\sigma^2}$, increases with the tax rate imposed by policymakers on speculators' capital gains, via the above-mentioned reduction of the risk premium $(1-\tau)^2\Delta$. Since, by construction, Z^* must remain constant and equal to $\bar{S}$ for any tax rate τ, an increase in τ necessarily implies – via the relation $Z^* = \bar{S}$ – an increase in P^* such that $P^* = \frac{\bar{D}-(1-\tau)^2\Delta}{r} = P^v$. Hence, the speculative demand pressure induced by higher capital gains taxes is offset by higher prices.

- Since $Det_l = \frac{(1-\tau)\chi}{1+r-\tau} < Det_u = \frac{\chi}{1+r}$, stability condition (15) is more binding than stability condition (22), i.e. the real fixed point becomes unstable before the virtual fixed point becomes unstable as the interest rate parameter r decreases or the extrapolation parameter χ increases. The same is true for the inequality that marks their transition from a stable node to a stable focus.

As we will see in the sequel, the transition of real and virtual fixed points from a stable node to a stable focus and their eventual loss of stability play a crucial role in the behavior of the model's complete map C. In Figure 1, we thus depict conditions (15), (16), (22) and (23) in (χ, r)-parameter space, setting $\tau = 0$ (red, real fixed point) and $\tau = 0.35$ (blue, virtual fixed point), subdividing the parameter space into seven distinct regions. For $\tau = 0$, parameter combinations from Regions R1, R2 and R3 imply that the price of the risky asset approaches its fundamental value, while parameter combinations from Regions R4, R5a, R5b and R5c imply divergent price paths. In the following, we show that parameter combinations from Region R3 may yield endogenous cyclical dynamics for $\tau > 0$, an outcome that highlights the potentially destabilizing nature of capital gains taxes. Note that

[7] A further implication of the relation $P^v > F$ is that the return of the risky asset at the virtual fixed point, say $\rho^v = \frac{\bar{D}}{P^v} = \frac{r}{1-(1-\tau)^2\lambda\sigma^2\bar{S}/\bar{D}}$, is smaller than its return at the real fixed point, namely $\rho^F = \frac{\bar{D}}{F} = \frac{r}{1-\lambda\sigma^2\bar{S}/\bar{D}}$. Moreover, the return of the risky asset at the virtual fixed point decreases with the tax rate imposed on capital gains, shifting P^v upwards.

the borders of Region R3 depend only on parameters χ and r, i.e. the size and existence of the area of Region R3 are independent of the tax rate imposed on speculators' capital gains taxes.[8] However, Regions R1 and R2 may also give rise to significant asset-price fluctuations induced by capital gains taxes, provided that the dynamics is subject to occasional small shocks. Interestingly, a small part of Region R4 yields bounded dynamics, although the price of the risky asset would be divergent in the absence of capital gains taxes. Hence, there is a small chance that capital gains taxes may indeed have a stabilizing effect on the dynamics of risky asset markets, as intended by policymakers, although the parameter space that guarantees such a stabilizing effect seems to us to be negligible. In Regions R5a, R5b and R5c, we always encounter diverging asset price dynamics.

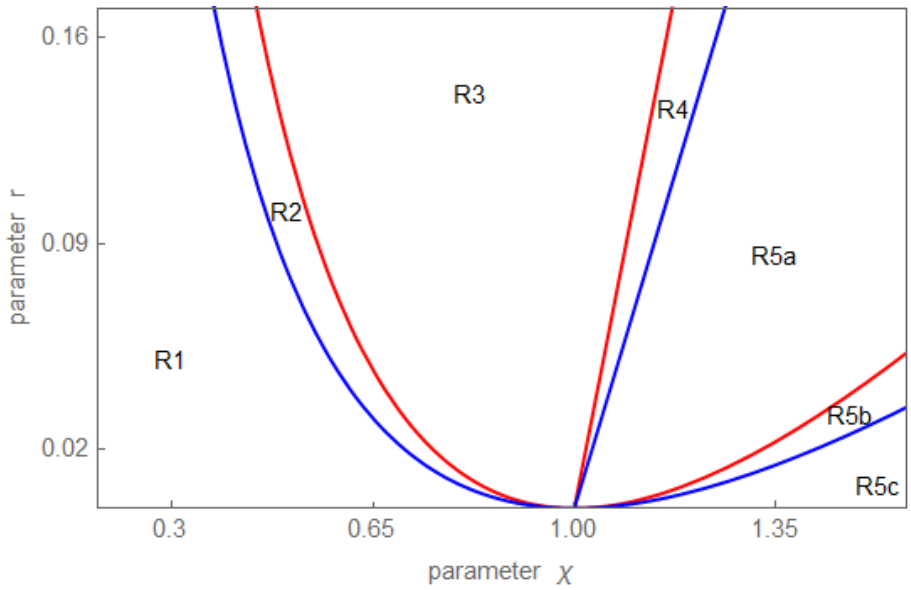

Figure 1: Regions in (χ, r)-parameter space. The panel shows the conditions for stability versus instability and node versus focus for the model's real and virtual fixed points, assuming $\tau = 0$ (red, real fixed point) and $\tau = 0.35$ (blue, virtual fixed point), subdividing the parameter space into seven distinct regions.

Before we continue, a few additional comments on our choice of model parameters in the remainder of our paper are in order. First, our parameter selection for each of the different regions we discuss seeks to optimally visualize our results. Second, taxes on capital gains may be quite substantial in actual markets, which is why we consider tax rates up to 35

[8] Obviously, higher tax rates increase the size of the area of Regions R2 and R4 at the expense of Regions R1 and R5a, respectively.

percent. See Littlewood and Elliffe (2017) for an international comparison of how countries tax capital gains. Third, exploring laboratory data from asset-pricing experiments, Hommes et al. (2005), Heemeijer et al. (2009) and Anufriev and Hommes (2012) conclude that human agents follow simple extrapolative expectation rules, as specified by (4), with extrapolation parameters ranging between 0.4 and 1.3. Hence, all regions depicted in Figure 1 are of relevance and need our attention.

3.2 Region R1

In Region R1, both the real fixed point and the virtual fixed point attract the price of the risky asset and possess a basin of attraction with positive measure. While both fixed points cannot be called "attractors" in the usual topological sense – there are points in their neighborhood that belong to the basin of attraction of the other fixed point – they may be regarded as Milnor attractors (Milnor 1985). As an example, Figure 2 shows the basin of attraction of the real fixed point F (in red) and the basin of attraction of the virtual fixed point P^v (in blue) for the parameter setting $\bar{D} = 0.2$, $\lambda\sigma^2\bar{S} = 0.1$, $r = 0.05$, $\chi = 0.3$ and $\tau = 0.35$. The figure also shows the path of two trajectories of the price of the risky asset, one converging towards the real fixed point $F = 2$ and the other towards the virtual fixed point $P^v \approx 3.16$.

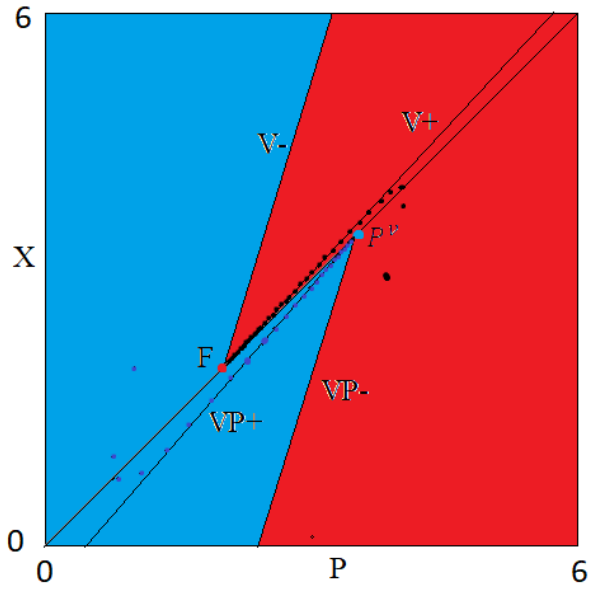

Figure 2: Example of the basins of attraction of the real fixed point F (red) and the virtual fixed point P^v (blue) for Region R1, together with the points of two trajectories. Parameter setting: $\bar{D} = 0.2$, $\lambda\sigma^2\bar{S} = 0.1$, $r = 0.05$, $\chi = 0.3$ and $\tau = 0.35$, implying that $F = 2$ and $P^v \approx 3.16$.

In the following, we first state and prove our main analytical results with respect to Region R1, and then comment on their economic implications.

Proposition (R1). *In Region R1, the basins of attraction of the real fixed point F and the virtual fixed point P^v are separated by the segment connecting (F, F) and (P^v, P^v), the upper eigenvector V_- issuing from the real fixed point F, and the lower eigenvector VP_- issuing from the virtual fixed point P^v.*

Proof: For parameters that belong to Region R1, the real fixed point F and the virtual fixed point P^v are attracting nodes with two positive eigenvalues, and $F < P^v$. It is clear from the equations of the eigenvalues and eigenvectors of the real fixed point F that the trajectories converge to the real fixed point F in the upper region of the (P, X)-phase plane, close to the half-line of eigenvector V_+ (associated with the highest positive eigenvalue). Points on the right side of eigenvector V_- in the upper half-plane have a trajectory converging to the real fixed point F. Points on the left side of eigenvector V_- in the upper half-plane (tending to the lower half-line of V_+) have a trajectory which enters the lower half-plane, and thus ultimately converge to the virtual fixed point P^v, tangentially to VP_+. A similar reasoning reveals that points below the diagonal on the left side of eigenvector VP_- converge to the virtual fixed point P^v, while those on the right converge to the real fixed point F.□

Figure 3, based on the same parameter setting as Figure 2, illustrates a number of economic implications associated with parameter combinations that belong to Region R1. The black line depicts the evolution of the risky asset price for 200 time steps, the blue line marks its real fixed point $F = 2$ and the green line stands for its virtual fixed point $\bar{P}^v \approx 3.16$. In addition, we assume that small exogenous shocks hit the risky asset market every 40 periods. Initially, due to a positive shock in period 1, the risky asset price monotonically moves towards its virtual fixed point $\bar{P}^v \approx 3.16$. After a negative shock in period 40, however, the real fixed point $F = 2$ attracts the price of the risky asset, until a further positive shock in period 80 reverses the path of the risky asset price once again. Recall that in the absence of capital gains taxes, the real fixed point would be globally stable and monotonically attract the price of the risky asset. Obviously, tiny infrequent shocks may –

in the presence of capital gains taxes – create pronounced swings in the price of the risky asset that are, on average, located above its fundamental value. Clearly, this is not in the interest of policymakers seeking to stabilize the dynamics of financial markets.

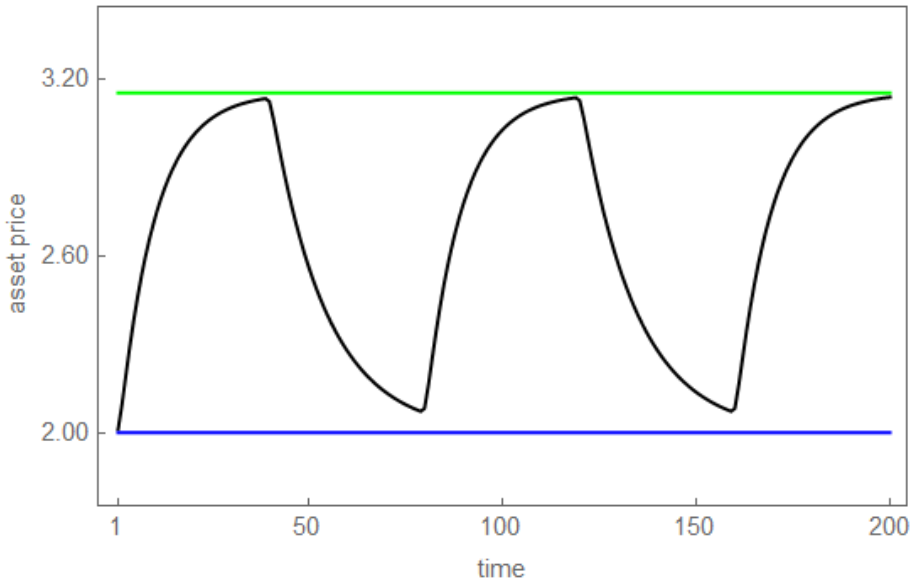

Figure 3: Time series dynamics of the risky asset price for Region R1. The black, blue and green lines show the evolution of the risky asset price, its real fixed point $F = 2$ and its virtual fixed point $P^v \approx 3.16$, respectively. Parameter setting: $\bar{D} = 0.2,\ \lambda\sigma^2\bar{S} = 0.1,\ r = 0.05,\ \chi = 0.3$ and $\tau = 0.35$. Tiny exogenous shocks hit the dynamics in periods 1, 40, 80, 120 and 160.

3.3 Region R2

With respect to the parameter space that belongs to Region R2, we are able to state the following result.

Proposition (R2). *In Region R2, the real fixed point F is globally attracting (in a topological sense).*

Proof: For parameters that belong to Region R2, the real fixed point F is an attracting node with two positive eigenvalues, while the virtual fixed point P^v is an attracting focus, and $F < P^v$. It follows that any point below the diagonal $X = P$ in the (P, X)-phase plane has a trajectory that – in order to converge to the virtual fixed point P^v – enters the region above this diagonal in a rotating manner in a finite number of steps, from which the trajectory monotonically converges to the real fixed point F.□

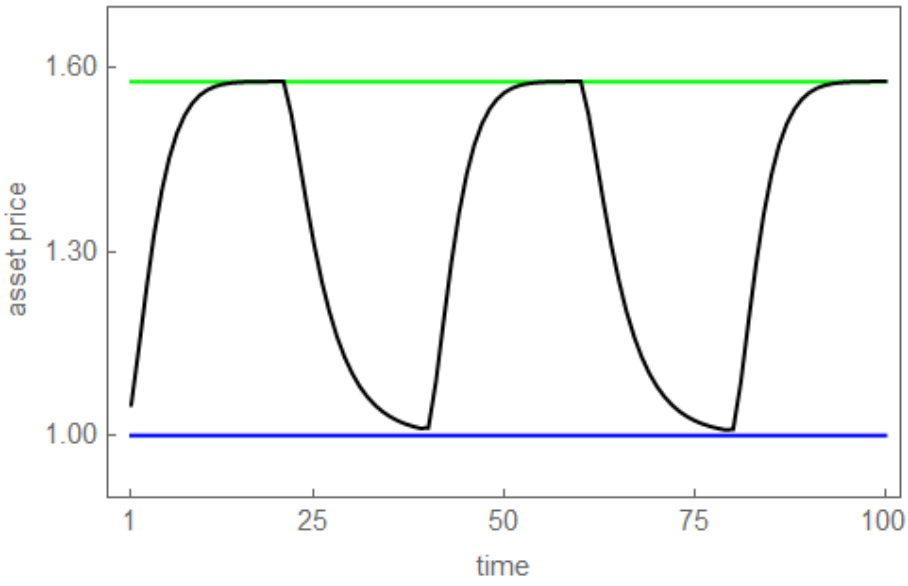

Figure 4: Time series dynamics of the risky asset price for Region R2. The black, blue and green lines show the evolution of the risky asset price, its real fixed point $F = 1$ and its virtual fixed point $P^v \approx 1.58$, respectively. Parameter setting: $\overline{D} = 0.2$, $\lambda\sigma^2\bar{S} = 0.1$, $r = 0.1$, $\chi = 0.5$ and $\tau = 0.35$. Tiny exogenous shocks hit the dynamics in periods 1, 40 and 80.

Despite being globally attracted (in a topological sense) by the real fixed point F, the price of the risky asset may nevertheless display surprisingly wild fluctuations. For instance, Figure 4 shows the development of the risky asset price for 100 periods, assuming the parameter setting $\overline{D} = 0.2$, $\lambda\sigma^2\bar{S} = 0.1$, $r = 0.1$, $\chi = 0.5$ and $\tau = 0.35$. The blue line marks the real fixed point $F = 1$ of the risky asset and the green line its virtual fixed point $P^v \approx 1.58$. Note that tiny exogenous shocks affect the risky asset market in periods 1, 40 and 80. After an initial (positive) shock in period 1, the price of the risky asset is about to converge towards its virtual fixed point $P^v \approx 1.58$. However, its oscillatory price path implies that the price of the risky asset must reverse its direction at some point. From then on, it monotonically moves towards its real fixed point F until the risky asset market is hit by the next (positive) shock in period 40. Recall that in the absence of capital gains taxes, the real fixed point would still be globally stable and would monotonically attract the price of the risky asset. Hence, the fluctuations we have just encountered are a consequence of capital gains taxes. In contrast to Region R1, we now observe that the price of the risky asset (slightly) overshoots its virtual steady state and does not necessitate a further

(negative) exogenous shock to reverse its direction.[9] Similar to Region R1, the price of the risky asset appears to be excessively volatile and, by fluctuating above its fundamental value, displays systematic mispricing.

3.4 Region R3

Our main results concern the dynamics of the model in Region R3. In particular, we are able to prove the following (surprising) statement.

Proposition (R3). *In Region R3, neither the real fixed point F nor the virtual fixed point P^v are attracting for the complete map C, despite being attracting foci for their respective sup-maps T_l and T_u.*

Proof: To prove this result, recall that both fixed points F and P^v are attracting foci of their respective sup-maps and located on the diagonal $X = P$ in the (P, X)-phase plane, the line at which the complete map C changes its definition. See panel (a) of Figure 5. Under sup-map T_l, the images of the real fixed point F belong to an arc of spiral up to a point in the upper region, intersecting the diagonal at point a. Under sup-map T_u, the images of the virtual fixed point P^v belong to an arc of spiral ending at a point below the diagonal, intersecting the diagonal at point b. Note that this point is mapped under sup-map T_l on points belonging to an arc of spiral up to the upper region, intersecting the diagonal at point $\mathrm{c} > \mathrm{a}$. Apparently, this leads to a neighborhood of the real fixed point F from which trajectories are escaping in a finite number of iterations, represented by the yellow region.□

While a complete characterization of the dynamics that occurs in Region R3 is beyond the scope of our paper, we can at least verify the existence of an attracting set. This is due to the fact that – although the dynamics close to the real fixed point F is necessary as described above, leading to an escape region EF – we can numerically observe the existence of a point A on the diagonal $X = P$ in the (P, X)-phase plane, with $\mathrm{A} > P^v$, whose images under map T_u belong to an arc of spiral up to a point below this diagonal (red point in panel (b) of Figure 5), after which map T_l applies up to a point above this diagonal (blue

[9] Stronger overshooting occurs for higher tax rates. However, it is clear that there is overshooting, followed by an endogenous reversal of the price direction, independently of the size of the (positive) tax rate.

point in panel (b) of Figure 5), located below the arc of spiral issuing from point A. This leads to a region AF that is attracting from outside and mapped into itself. It follows that the annular region $NF = AF \backslash EF$ is attracting and mapped into itself (indicated by the pink region in panel (b) of Figure 5). Thus, an attracting set must necessarily exist in the invariant set $\mathcal{A}$ defined as $\mathcal{A} = \cap_{n \geq 0} T^n(NF)$.[10] The fact that $\mathcal{A}$ includes at least an attracting cycle will be numerically demonstrated in the next four figures.

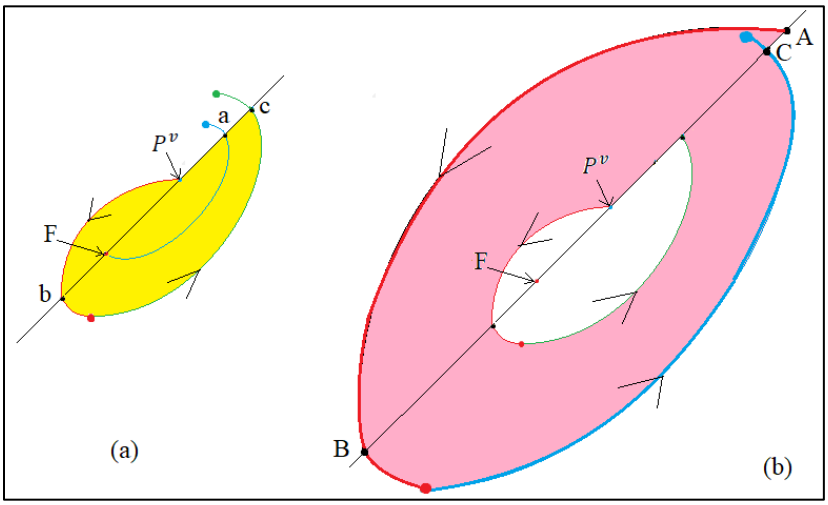

Figure 5: Qualitative sketch of escape regions and attracting sets in the (P, X)-phase plane for Region R3. The yellow area depicted in panel (a) visualizes a neighborhood of the real fixed point F from which trajectories are escaping in a finite number of iterations. The pink region depicted in panel (b) indicates a region that contains an attracting cycle.

To discuss the economic consequences associated with Region R3 in more detail, let us assume the following base parameter setting: $\overline{D} = 0.2$, $\lambda \sigma^2 \bar{S} = 0.1$, $r = 0.1$, $\chi = 0.9$ and $\tau = 0.01$. Figure 6 presents the evolution of the price of the risky asset in the time domain for $\tau = 0.01$ (black) and $\tau = 0$ (red). The corresponding real fixed point $F = 1$ and the virtual fixed point $P^v \approx 1.02$, both being stable foci, are plotted in blue and green, respectively. In the absence of capital gains taxes, the dynamics of the model is globally stable, i.e. the price of the risky asset oscillates around its fundamental value with decreasing amplitude and reaches its fundamental value after about 40 periods. In contrast, everlasting cyclical asset price dynamics emerge for $\tau = 0.01$.

[10] Besides containing an attracting cycle, this set may also include coexisting attracting cycles.

To understand the functioning of the model in Region R3, we reiterate that cyclical asset price motion implies that the risky asset market either goes up or down, i.e. there are two (competing) regimes:

- Regime 1 (no capital gains taxes): When the price of the risky asset decreases, speculators expect not to have to pay capital gains taxes. Consequently, the dynamics is driven by sub-map T_u, setting a cyclical convergence towards $F = (\bar{D} - \lambda\sigma^2\bar{S})/r$ in motion. However, a cyclical convergence means that the downward movement of the price of the risky asset continues for a while, but then changes direction. Importantly, this triggers a regime change.
- Regime 2 (capital gains taxes): When the price of the risky asset eventually goes up, speculators expect to have to pay capital gains taxes. Then, sup-map T_l and its virtual fixed point, $\bar{P}^v = \frac{\bar{D}-(1-\tau)^2\lambda\sigma^2\bar{S}}{r} > F$, determine the fate of the dynamics, at least for a while. Of course, the cyclical adjustment path of the price of the risky asset implies that a downturn will eventually occur, such that the other sub-map becomes relevant again.

Hence, the dynamics of the risky asset market is kept alive by the constant switching between regimes (i) and (ii), i.e. speculators' alternating beliefs about the future direction of the risky asset market and their associated beliefs about their tax duties.

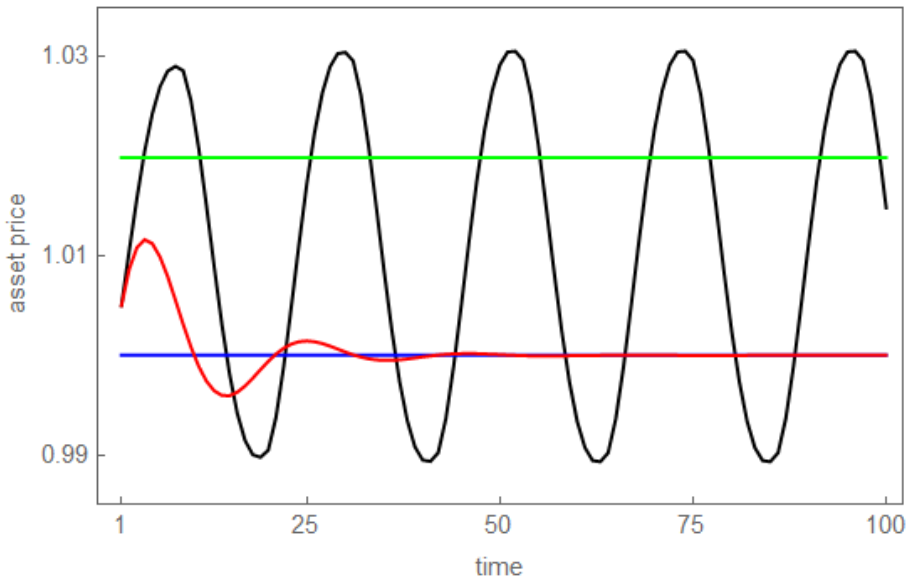

Figure 6: Time series dynamics of the risky asset price in Region R3. The black, blue and green lines show the evolution of the risky asset price, its real fixed point $F = 1$ and its virtual fixed point $P^v \approx 1.02$, respectively. Parameter setting: $\bar{D} = 0.2$, $\lambda\sigma^2\bar{S} = 0.1$, $r = 0.1$, $\chi = 0.9$ and $\tau = 0.01$. The red line shows the evolution of the risky asset price for $\tau = 0$.

Note that the emergence of such regime-dependent asset price fluctuations are independent of the size of the risky asset's risk premium, and thus of parameters λ, σ^2 and $\bar{S}$. While both the size of the risk premium and the tax rate imposed by policymakers on speculators' capital gains affect the distance between the real and the virtual fixed point of the risky asset price and therefore the amplitude of its oscillatory price motion, it is not crucial for the emergence of such dynamics.[11] Since the price of the risky asset oscillates around the fixed points F and P^v, it is furthermore clear that the average price level of the risky asset gets upward biased, i.e. capital gains taxes do not only generate excess volatility, but also systematic mispricing, an outcome that Blouin et al. (2003), Jin (2006), George and Hwang (2007) and Jacob (2018) have also found for actual asset markets that are subject to capital gains taxes.[12]

The bifurcation diagram depicted in Figure 7 rests on our base parameter setting for Region R3, except that we vary parameter τ as indicated on the axis. Apparently, a tax imposed on speculators' capital gains has a destabilizing impact on the dynamics of the model. In particular, we observe the emergence of endogenous dynamics immediately when parameter τ becomes positive. Moreover, the risky asset's volatility, average price and (systematic) mispricing increase in line with the tax rate imposed by policymakers on speculators' capital gains. Note also that the periodicity of the cycles may change as parameter τ increases.

Figure 8 shows a bifurcation diagram for the base parameter setting of Region R3 in which we vary parameter χ as indicated on the axis. Note that the risky asset price converges towards its real fixed point $F = 1$ for $\chi < 0.537$, as can be computed from (16). As parameter χ enters Region R3, however, the price of the risky asset abruptly displays cycles with significant amplitudes. Similar to the dynamics depicted in Figure 7, the price of the risky asset is excessively volatile and fluctuates, on average, above its real fixed point. Clearly, the volatility and mispricing of the risky asset display a discrete jump as speculators' trend extrapolation strength exceeds the critical bifurcation value $\chi = 0.537$.

[11] We stress this point to make it clear that it is irrelevant whether speculators' risk perception, which we fixed to $V_t^i[P_{t+1}] = \sigma^2$ in Section 2, is accurate or not. What really matters here is that there are two coexisting fixed points, one real and one virtual, both of which are stable foci.

[12] Note that the dynamics we observe in Regions 1 and 2 are also associated with inflated price levels.

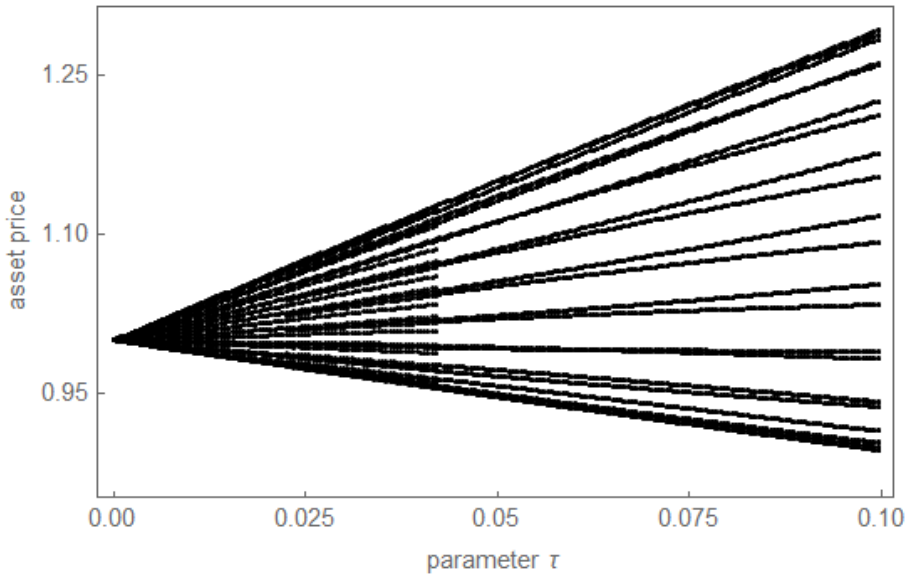

Figure 7: Bifurcation diagram for parameter τ. The panel shows how the price of the risky asset reacts to an increase in the tax rate on capital gains. Base parameter setting for Region R3, except that parameter τ is varied as indicated on the axis.

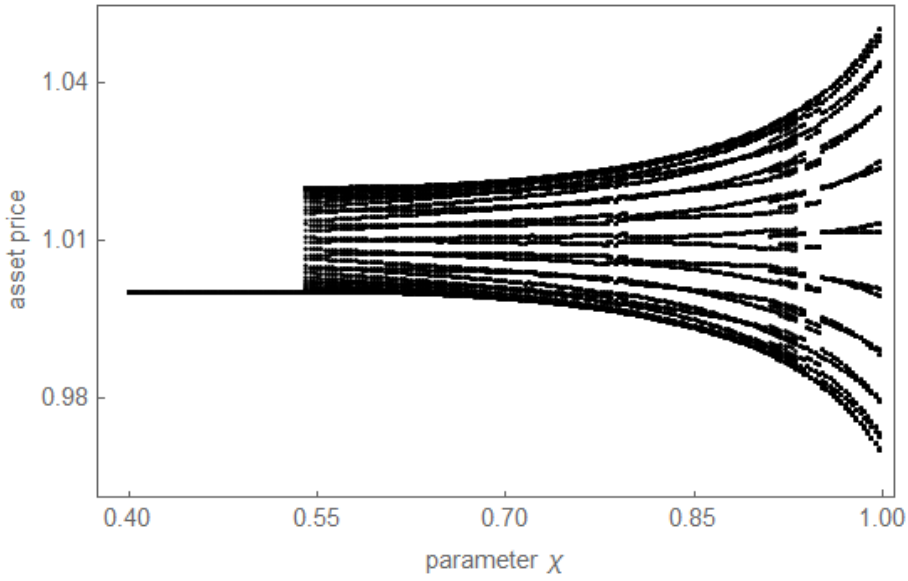

Figure 8: Bifurcation diagram for parameter χ. The panel shows how asset prices react to an increase in speculators' extrapolation strength. Base parameter setting for Region R3, except that parameter χ is varied as indicated on the axis.

Figure 8 reveals that the periodicity of the risky asset's price cycles may change as parameter χ increases. To delve deeper into this issue, we present in Figure 9 a two-dimensional bifurcation diagram in which we vary parameters r and χ as indicated on the

axis (the remaining parameters are as in our base parameter setting for Region R3, except that $\tau = 0.35$). Note that different colors indicate different periodicities. It is immediately apparent from the superimposed bifurcation curves (15), (16), (22) and (23) that Region R3 is filled with cycles of different length (for clarity, see Figure 2, also based on $\tau = 0.35$). Without going into too much detail, we remark that the periods of the attracting cycles change due to border collision bifurcations associated with the cycles. In other words, a border collision bifurcation, changing the period of a cycle, occurs when a periodic point of an attracting cycle merges with the diagonal $X = P$ in the (P, X)-phase plane, either from above or from below. The yellow area in the left part of the bifurcation diagram stands for fixed-point dynamics, occurring in Regions R1 and R2, while the gray area in the right part of the bifurcation diagram indicates divergent dynamics, occurring in large parts of Region R4 and throughout Regions R5a, R5b and R5c.

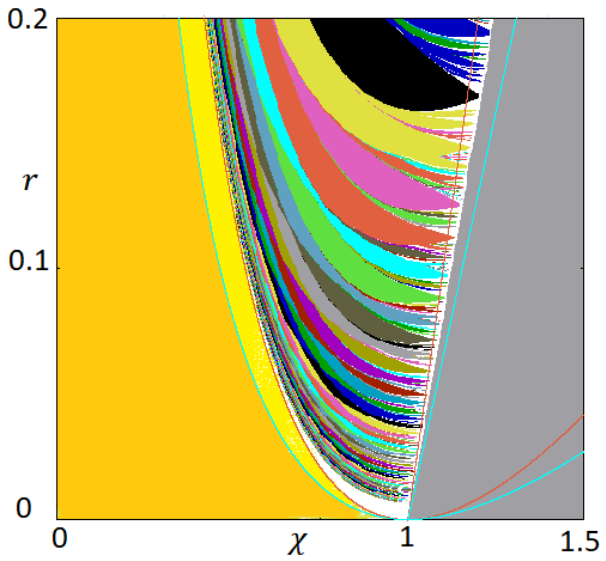

Figure 9: Two-dimensional bifurcation diagram for parameters r and χ. Different colors denote cycles with different periods. The yellow (gray) area in the left (right) part of the bifurcation diagram stands for fixed-point (divergent) dynamics. Bifurcation curves (15), (16), (22) and (23) have been superimposed. Base parameter setting for Region R3, except that $\tau = 0.35$; parameters r and χ are varied as indicated on the axis.

3.4 Regions R4 and R5

What is remarkable is that we may also detect attracting cycles in Region R4 – a region in which the real fixed point F is an expanding focus, but the virtual fixed point P^v is still

an attracting focus – at least as long as the parameters are close to the bifurcation curve (16) of the real fixed point F. We are able to explain this puzzling outcome as follows. When the real fixed point F becomes unstable, it is locally repelling, and a region EF can be constructed as described above. However, as long as it is possible to find a point A on the diagonal $X = P$ in the (X, P)-phase plane whose images belong to two arcs of spirals ending at a point below the initial arc issuing from A, as described in panel (b) of Figure 5, then an annular absorbing region exists, leading to an attracting set.

An example of such an outcome is shown in Figure 10, resting on $\bar{D} = 2.6$, $\lambda\sigma^2\bar{S} = 0.1$, $r = 0.1$, $\chi = 1.11$ and $\tau = 0.3$. As can be seen, the price of the risky asset fluctuates around $\bar{P} = 25$ (blue) and $P^v \approx 25.5$ (green), and does not explode as it would for $\tau = 0$. It is therefore possible, in principle, that capital gains taxes will stabilize the dynamics of financial markets, as intended by policymakers. Unfortunately, the parameter space that guarantees such dynamics appears to us to be relatively small. Moreover, we consider the associated amplitudes of the cycles to be generally quite large. Of course, it may be argued that such a volatile outcome is better than divergent dynamics.

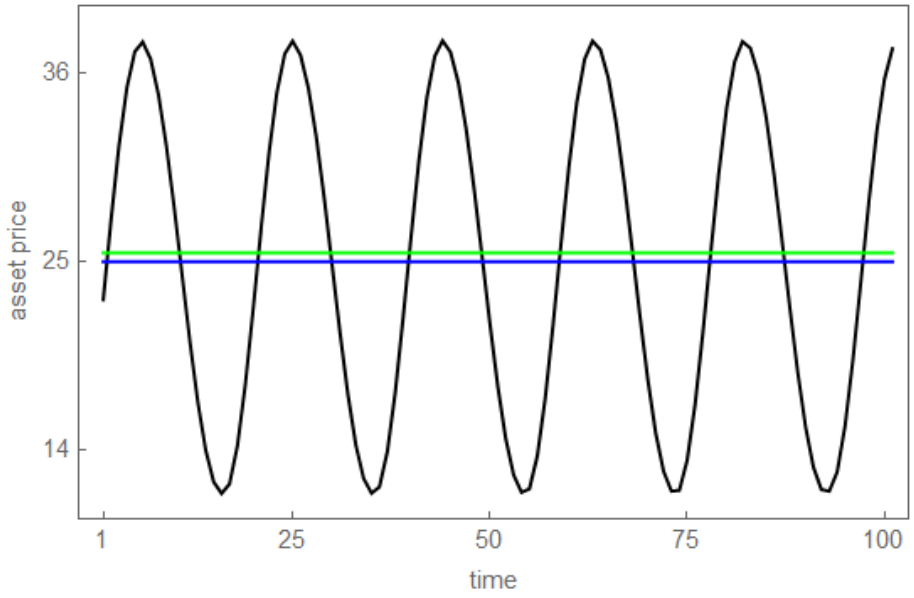

Figure 10: Time series dynamics of risky asset prices in Region R4. The black, blue and green lines show the risky asset price, its real fixed point $\bar{P} = 25$ and its virtual fixed point $P^v \approx 25.5$, respectively. Parameter setting: $\bar{D} = 2.6$, $\lambda\sigma^2\bar{S} = 0.1$, $r = 0.1$, $\chi = 1.11$ and $\tau = 0.3$.

As the parameters change in Region R4 such that any point A on the diagonal has a trajectory belonging to two arcs of spirals ending above the initial arc, all trajectories are divergent. This is what occurs in Region R5a, when the real fixed point F and the virtual fixed point P^v are repelling foci. In this region, any initial condition different from the real fixed point F has a trajectory spiraling away from the real fixed point F and the virtual fixed point P^v, and is thus divergent. Moreover, all parameter combinations in Region R5b (where the real fixed point F is a repelling node and the virtual fixed point P^v is a repelling focus) and in Region R5c (where the real fixed point F and the virtual fixed point P^v are both repelling nodes) cause divergent dynamics, too.

4 Robustness checks

We now show that our main results carry over to an asset-pricing model in which speculators consist of chartists, who rely on an extrapolative expectation rule, and fundamentalists, who use a regressive expectation rule. In Section 4.1, we keep the market shares of chartists and fundamentalists constant. In Section 4.2, we consider that speculators endogenously switch between an extrapolative and a regressive expectation rule, subject to an evolutionary fitness measure, as in Brock and Hommes (1998).[13] Due to our model extensions, the price of the risky asset is driven by piecewise maps with four branches, which are either linear or nonlinear. Since these maps preclude a deeper analytical penetration, we focus our attention on numerical investigations.

4.1 Chartists and fundamentalists: constant market shares

Let us again assume that a chartist applies the extrapolative expectation rule

$$E_t^C[P_{t+1}] = P_{t-1} + \chi(P_{t-1} - P_{t-2}), \tag{27}$$

with extrapolation parameter $\chi > 0$, and that his risky asset demand is given by

$$Z_t^C = \begin{cases} \frac{(1-\tau)E_t^C[P_{t+1}]+\bar{D}-(1+r-\tau)P_t}{(1-\tau)^2\lambda\sigma^2} & if\ P_{t-1} - P_{t-2} > 0 \\ \frac{E_t^C[P_{t+1}]+\bar{D}-(1+r)P_t}{\lambda\sigma^2} & if\ P_{t-1} - P_{t-2} \leq 0 \end{cases}. \tag{28}$$

[13] Martin et al. (2021) provide preliminary simulations on how capital gains taxes may affect the dynamics of a housing market model, assuming that speculators switch between heterogeneous expectation rules, subject to an evolutionary fitness measure.

A fundamentalist believes that the price of the risky asset will move towards $F = \frac{\bar{D}-\lambda\sigma^2\bar{S}}{r}$.

Let us capture the regressive expectation rule of fundamentalists by

$$E_t^F[P_{t+1}] = P_{t-1} + \phi(F - P_{t-1}), \tag{29}$$

with mean reversion parameter $0 < \phi \leq 1$. Consistent with this expectation rule, a fundamentalist's risky asset demand results in

$$Z_t^F = \begin{cases} \frac{(1-\tau)E_t^F[P_{t+1}]+\bar{D}-(1+r-\tau)P_t}{(1-\tau)^2\lambda\sigma^2} & if\ F - P_{t-1} > 0 \\ \frac{E_t^F[P_{t+1}]+\bar{D}-(1+r)P_t}{\lambda\sigma^2} & if\ F - P_{t-1} \leq 0 \end{cases}. \tag{30}$$

Clearly, a fundamentalist believes that he need (not) pay capital gains taxes when the risky asset is currently undervalued (overvalued), projecting a price recovery (decline).

Let $0 < n^C < 1$ and $n^F = 1 - n^C$ stand for the constant market shares of chartists and fundamentalists, respectively, and let N denote the total number of speculators. Speculators' aggregate demand for the risky asset then amounts to

$$Z_t = N(n^C Z_t^C + n^F Z_t^F). \tag{31}$$

As before, market equilibrium requires that

$$Z_t = S_t, \tag{32}$$

where the supply of the risky asset is set to

$$S_t = \hat{S} = N\bar{S}. \tag{33}$$

Combining (27) to (33) reveals that the price of the risky asset adheres to

$$P_t = \begin{cases} \frac{(1-\tau)(n^C E_t^C[P_{t+1}]+n^F E_t^F[P_{t+1}])+\bar{D}-(1-\tau)^2\lambda\sigma^2\bar{S}}{1+r-\tau} & if\ P_{t-1} > P_{t-2}\ \wedge F > P_{t-1} \\ \frac{(1-\tau)n^C E_t^C[P_{t+1}]+n^C\bar{D}+(1-\tau)^2 n^F(E_t^F[P_{t+1}]+\bar{D})-(1-\tau)^2\lambda\sigma^2\bar{S}}{n^C(1+r-\tau)+(1-\tau)^2 n^F(1+r)} & if\ P_{t-1} > P_{t-2}\ \wedge F \leq P_{t-1} \\ \frac{(1-\tau)^2 n^C(E_t^C[P_{t+1}]+\bar{D})+(1-\tau)n^F E_t^F[P_{t+1}]+n^F\bar{D}-(1-\tau)^2\lambda\sigma^2\bar{S}}{(1-\tau)^2 n^C(1+r)+n^F(1+r-\tau)} & if\ P_{t-1} \leq P_{t-2}\ \wedge F > P_{t-1} \\ \frac{n^C E_t^C[P_{t+1}]+n^F E_t^F[P_{t+1}]+\bar{D}-\lambda\sigma^2\bar{S}}{1+r} & if\ P_{t-1} \leq P_{t-2}\ \wedge F \leq P_{t-1} \end{cases}, \tag{34}$$

i.e. its dynamics depends on the interaction of four linear branches.

In the absence of capital gains taxes, the dynamics of the model obeys

$$R: \begin{cases} P_t = \frac{P_{t-1}+n^C\chi(P_{t-1}-X_{t-1})+n^F\phi(F-P_{t-1})+\bar{D}-\lambda\sigma^2\bar{S}}{1+r} \\ X_t = P_{t-1} \end{cases}, \tag{35}$$

where $X_t = P_{t-1}$ is an auxiliary variable. Note that map (35) possesses a unique fixed

point, given by $\bar{P} = \bar{X} = F = \frac{\bar{D} - \lambda\sigma^2\bar{S}}{r}$, which is globally stable if $\chi < \frac{1+r}{n^C}$ holds. In the presence of capital gains taxes, the dynamics of the model is due to

$$C: \begin{cases} P_t = \begin{cases} \frac{(1-\tau)((n^C(P_{t-1}+\chi(P_{t-1}-X_{t-1}))+n^F(P_{t-1}+\phi(F-P_{t-1})))+\bar{D}-(1-\tau)^2\lambda\sigma^2\bar{S}}{1+r-\tau} & if\ P_{t-1} > X_{t-1} \wedge F > P_{t-1} \\ \frac{(1-\tau)n^C(P_{t-1}+\chi(P_{t-1}-X_{t-1}))+n^C\bar{D}+(1-\tau)^2n^F(P_{t-1}+\phi(F-P_{t-1})+\bar{D})-(1-\tau)^2\lambda\sigma^2\bar{S}}{n^C(1+r-\tau)+(1-\tau)^2n^F(1+r)} & if\ P_{t-1} > X_{t-1} \wedge F \leq P_{t-1} \\ \frac{(1-\tau)^2n^C(P_{t-1}+\chi(P_{t-1}-X_{t-1})+\bar{D})+(1-\tau)n^F(P_{t-1}+\phi(F-P_{t-1}))+n^F\bar{D}-(1-\tau)^2\lambda\sigma^2\bar{S}}{(1-\tau)^2n^C(1+r)+n^F(1+r-\tau)} & if\ P_{t-1} \leq X_{t-1} \wedge F > P_{t-1} \\ \frac{P_{t-1}+n^C\chi(P_{t-1}-X_{t-1})+n^F\phi(F-P_{t-1})+\bar{D}-\lambda\sigma^2\bar{S}}{1+r} & if\ P_{t-1} \leq X_{t-1} \wedge F \leq P_{t-1} \end{cases} \\ X_t = P_{t-1} \end{cases} \quad (36)$$

In the following, we first present a simulation run of the model, indicating that the imposition of capital gains taxes may create endogenous asset price dynamics. We then present a two-dimensional bifurcation diagram suggesting that map (36) may produce similar dynamics to those of map (9).

For the time series example, we assume that $r = 0.1$, $\bar{D} = 0.2$, $\lambda\sigma^2\bar{S} = 0.1$, $n^C = 0.8$, $\chi = 0.9$ and $\phi = 0.6$, implying that $F = 1$ and $n^F = 0.2$. Moreover, the risky asset market is subject to a small exogenous shock in period $t = 1$. As revealed by the red line in Figure 11, the price of the risky asset quickly converges towards $F = 1$ for $\tau = 0$. However, endogenous cyclical asset price dynamics emerges for $\tau = 0.02$, as evidenced by the black line. We note that while we face interactions between upward and downward trending regimes in the model with chartists, we now encounter four interdependent regimes in the model with chartists and fundamentalists. In fact, it can easily be verified that in the course of the asset price cycles depicted in Figure 11, we have that (i) the risky asset market increases and is overvalued, (ii) the risky asset market decreases and is overvalued, (iii) the risky asset market decreases and is undervalued and (iv) the risky asset market increases and is undervalued. Thus, all four linear branches of map (36) are relevant and visited repeatedly, implying that all of their fixed points, whether real or virtual, and their stability properties matter for the dynamics.

A comparison of the two-dimensional bifurcation diagrams presented in Figures 9 and 12 reveals that maps (9) and (36) produce similar dynamics. The underlying parameter setting for Figure 12 is given by $\bar{D} = 0.2$, $\lambda\sigma^2\bar{S} = 0.1$, $\tau = 0.35$, $n^C = 0.8$, $n^F = 0.2$ and $\phi = 0.6$, while parameters r and χ are varied as indicated on the axis. With some liberty, we can conclude that both models produce fixed-point (divergent) dynamics when chartists'

extrapolation parameter is relatively low (high), as indicated by the yellow (gray) area in the bottom left (right) part of the bifurcation diagrams. For intermediate values of parameter χ, periodic motion with cycles that have different periods emerge, as indicated by the different colors in the center part of the bifurcation diagram. Since the model with chartists and fundamentalists depends on four rather than two branches, the areas where cycles change their periods appear more ragged. Qualitatively, however, there is a strong similarity between Figures 9 and 12.

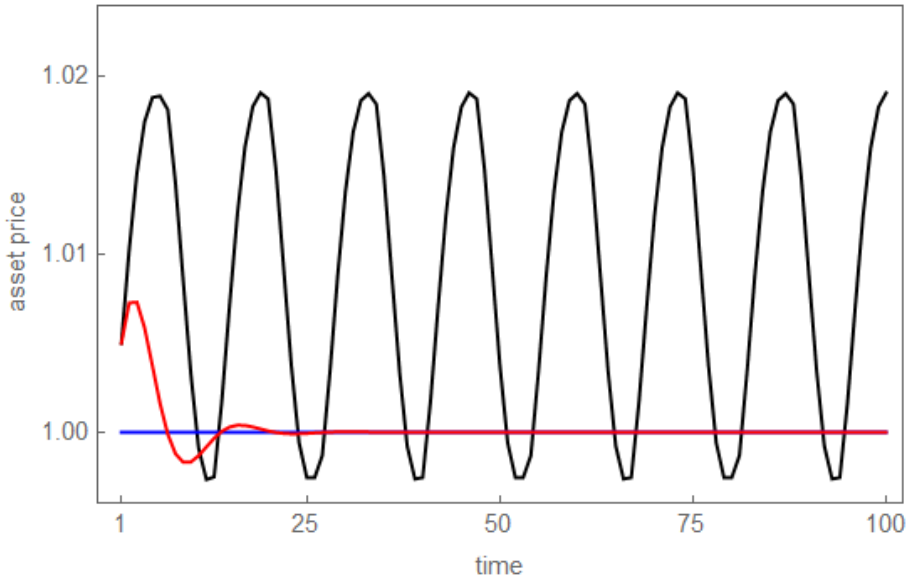

Figure 11: Time series dynamics of the risky asset price for the model with constant market shares of chartists and fundamentalists. The black line shows the evolution of the risky asset price, assuming $\overline{D} = 0.2$, $\lambda\sigma^2\bar{S} = 0.1$, $r = 0.1$, $\tau = 0.02$, $n^C = 0.8$, $\chi = 0.9$, $n^F = 0.2$ and $\phi = 0.6$. The red line depicts the evolution of the risky asset price for the same parameter setting, except that $\tau = 0$. The blue line marks $F = 1$.

4.2 Chartists and fundamentalists: endogenous market shares

In this section, we assume that speculators display a boundedly rational learning behavior, as put forward by Brock and Hommes (1998). Accordingly, speculators choose between an extrapolative and a regressive expectation rule to forecast the price of the risky asset subject to an evolutionary fitness measure, given by the prediction accuracy of the expectation rules. With a view to the omnipresent wilderness-of-bounded-rationality critique, Glaeser (2013) and Hommes (2013) stress that a simple and plausible rule-governed expectation formation scheme describes reality more accurate than a framework with fully rational expectations.

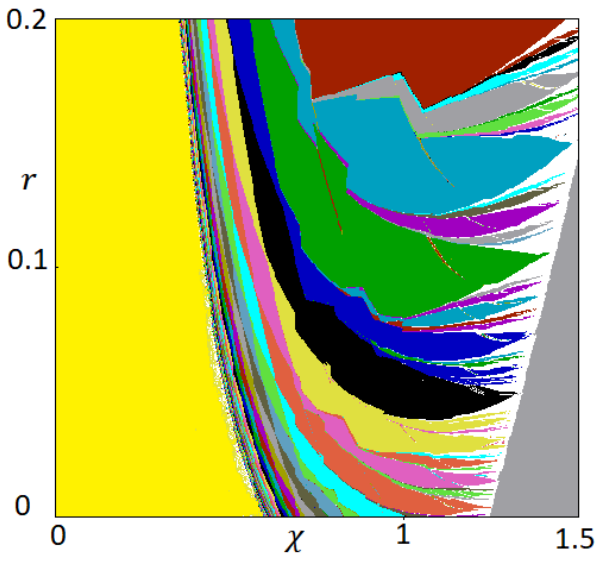

Figure 12: Two-dimensional bifurcation diagram for parameters r and χ. Different colors denote cycles with different periods. The yellow (gray) area in the left (right) part of the bifurcation diagram stands for fixed-point (divergent) dynamics. Parameters r and χ are varied, as indicated on the axis. Remaining parameters: $\bar{D} = 0.2$, $\lambda\sigma^2\bar{S} = 0.1$, $\tau = 0.35$, $n^C = 0.8$, $n^F = 0.2$ and $\phi = 0.6$.

As a starting point, we use price equation (34) of the model developed in Section 4.1, except that we now consider that the market shares of chartists and fundamentalists, i.e. n_t^C and n_t^F, evolve over time. We thus have

$$P_t = \begin{cases} \frac{(1-\tau)(n_t^C E_t^C[P_{t+1}]+n_t^F E_t^F[P_{t+1}])+\bar{D}-(1-\tau)^2\lambda\sigma^2\bar{S}}{1+r-\tau} & if\ P_{t-1} > P_{t-2} \wedge F > P_{t-1} \\ \frac{(1-\tau)n_t^C E_t^C[P_{t+1}]+n_t^C\bar{D}+(1-\tau)^2 n_t^F(E_t^F[P_{t+1}]+\bar{D})-(1-\tau)^2\lambda\sigma^2\bar{S}}{n_t^C(1+r-\tau)+(1-\tau)^2 n_t^F(1+r)} & if\ P_{t-1} > P_{t-2} \wedge F \leq P_{t-1} \\ \frac{(1-\tau)^2 n_t^C(E_t^C[P_{t+1}]+\bar{D})+(1-\tau)n_t^F E_t^F[P_{t+1}]+n_t^F\bar{D}-(1-\tau)^2\lambda\sigma^2\bar{S}}{(1-\tau)^2 n_t^C(1+r)+n_t^F(1+r-\tau)} & if\ P_{t-1} \leq P_{t-2} \wedge F > P_{t-1} \\ \frac{n_t^C E_t^C[P_{t+1}]+n_t^F E_t^F[P_{t+1}]+\bar{D}-\lambda\sigma^2\bar{S}}{1+r} & if\ P_{t-1} \leq P_{t-2} \wedge F \leq P_{t-1} \end{cases}. \quad (37)$$

At the beginning of each time step, speculators have to determine which expectation rule to follow. To model the evolution of the market shares of chartists and fundamentalists, Brock and Hommes (1998) employ the discrete choice approach, resulting in

$$n_t^C = \frac{exp[\beta A_t^C]}{exp[\beta A_t^C]+exp[\beta A_t^F]} \quad (38)$$

and

$$n_t^F = \frac{exp[\beta A_t^F]}{exp[\beta A_t^C]+exp[\beta A_t^F]}, \quad (39)$$

where A_t^C and A_t^F denote the fitness of the extrapolative and the regressive expectation

rule, respectively. Importantly, parameter $\beta > 0$ measures how quickly the mass of speculators switches to the fitter expectation rule. For $\beta \to 0$, speculators do not observe any fitness differentials between the two expectation rules, implying that $n_t^C = n_t^F = 0.5$. For $\beta \to \infty$, speculators observe fitness differentials perfectly, and all of them will choose the expectation rule that yields the higher fitness. Clearly, the higher parameter β is, the more speculators will select the fitter expectation rule.

The fitness of the two expectation rules depends on their prediction accuracy, modeled via their last observable (squared) prediction error. Hence,

$$A_t^C = -(P_{t-1} - E_{t-2}^C[P_{t-1}])^2 = -(P_{t-1} - P_{t-3} - \chi(P_{t-3} - P_{t-4}))^2 \quad (40)$$

and

$$A_t^F = -(P_{t-1} - E_{t-2}^F[P_{t-1}])^2 = -(P_{t-1} - P_{t-3} - \phi(F - P_{t-3}))^2, \quad (41)$$

respectively. Note that both expectation rules make no forecast error when the risky asset market is at rest, a constellation that yields $n_t^C = n_t^F = 0.5$.

Scrutiny of (37)-(41) reveals that the price of the risky asset is now due to a four-dimensional piecewise map with four nonlinear branches, which is why we explore its dynamics numerically. Figure 13 displays time series dynamics of the risky asset price and the market share of chartists that result from a small exogenous shock that hit the risky asset market in period $t = 1$. The black line in the top (bottom) panel shows the evolution of the risky asset price (market share of chartists), assuming $\overline{D} = 0.2$, $\lambda\sigma^2\overline{S} = 0.1$, $r = 0.1$, $\tau = 0.028$, $\chi = 0.9$, $\phi = 0.6$ and $\beta = 10{,}000$. The red line in the top (bottom) panel depicts the evolution of the risky asset price (market share of chartists) for the same parameter setting, except that $\tau = 0$. The blue line in the top (bottom) panel marks $F = 1$ ($\overline{n^C} = \overline{n^F} = 0.5$). We can conclude from this experiment that the price of the risky asset quickly approaches its fundamental value $F = 1$ when policymakers do not impose capital gains taxes. In contrast, the price of the risky asset is subject to endogenous cyclical price changes that occur around inflated price levels when speculators face capital gains taxes, as we have already witnessed in the previous sections of our paper.

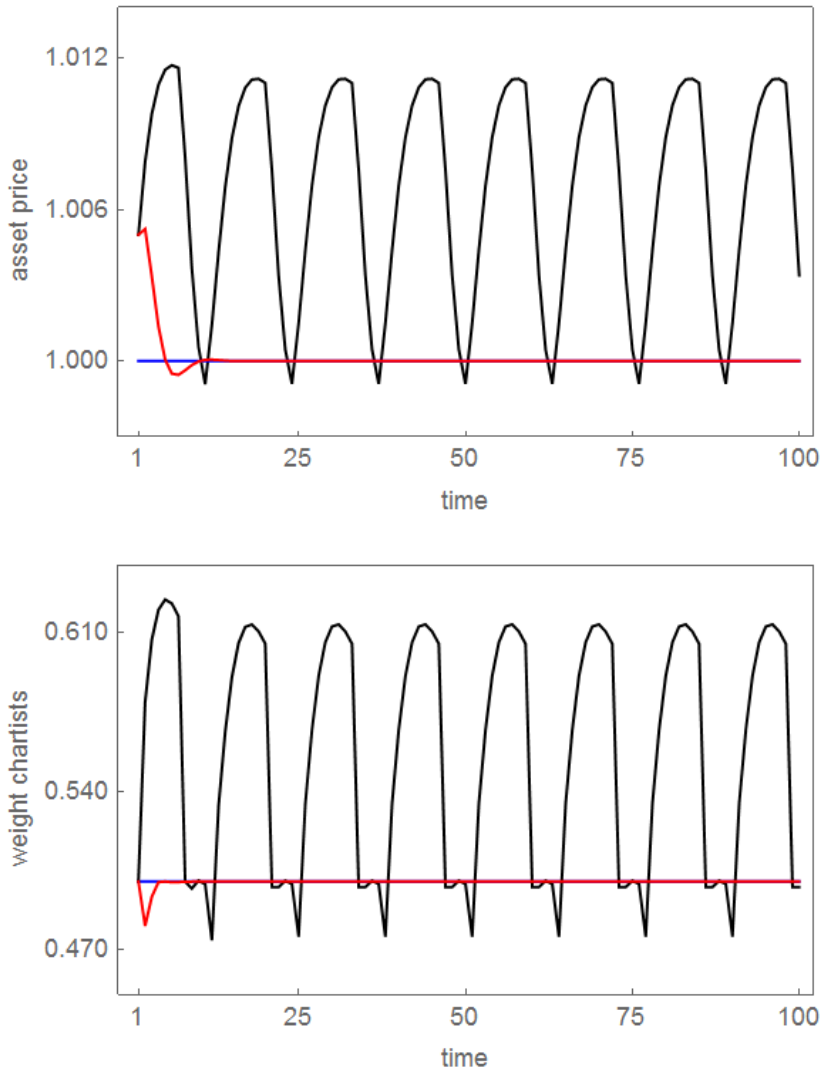

Figure 13: Time series dynamics of the risky asset price and the market share of chartists for the model with endogenous market shares of chartists and fundamentalists. The black line in the top (bottom) panel shows the evolution of the risky asset price (market share of chartists), assuming $\overline{D} = 0.2$, $\lambda\sigma^2\bar{S} = 0.1$, $r = 0.1$, $\tau = 0.028$, $\chi = 0.9$, $\phi = 0.6$ and $\beta = 10{,}000$. The red line in the top (bottom) panel depicts the evolution of the risky asset price (market share of chartists) for the same parameter setting, except that $\tau = 0$. The blue line in the top (bottom) panel marks $F = 1$ ($\overline{n^C} = \overline{n^F} = 0.5$).

Note also that speculators switch between the extrapolative and the regressive expectation rule. The extrapolative expectation rule becomes more popular when a bubble builds up, an outcome that tends to amplify the destabilizing effect of capital gains taxes. Fundamentalists briefly dominate the risky asset market when it crashes – during these

periods their predictions are more accurate than those of chartists. Of course, the price of the risky asset is now jointly determined by speculators' boundedly rational learning and expectation formation behavior and by policymakers' capital gains taxation. While it is difficult to disentangle the interactions between these two (destabilizing) components, it is clear that the risky asset market is stable for $\tau = 0$, at least for the current model parameterization. Against this background, we may conclude that the nature of capital gains taxes is destabilizing.

Let us try to generalize the latter observation. The left panel of Figure 14 reports the average price of the risky asset, defined as $\frac{1}{T}\sum_{t=1}^{T} P_t$, as a function of the tax rate. We assume the same parameter setting as in Figure 13, except that we gradually increase the tax rate from $\tau = 0$ to $\tau = 0.05$, as indicated on the axis. For each tax rate, we use $T = 10{,}000$ observations to compute the average price of the risky asset. As can be seen, the average price of the risky asset increases with the tax rate on capital gains. The right panel of Figure 14 displays the volatility of the risky asset, defined as $\frac{1}{T}\sum_{t=1}^{T} |P_t - P_{t-1}|$, with $T = 10{,}000$. Since the volatility of the risky asset also increases with the tax rate, we may conclude that capital gains taxes destabilize the dynamics of the risky asset market, even when speculators display a boundedly rational learning behavior.

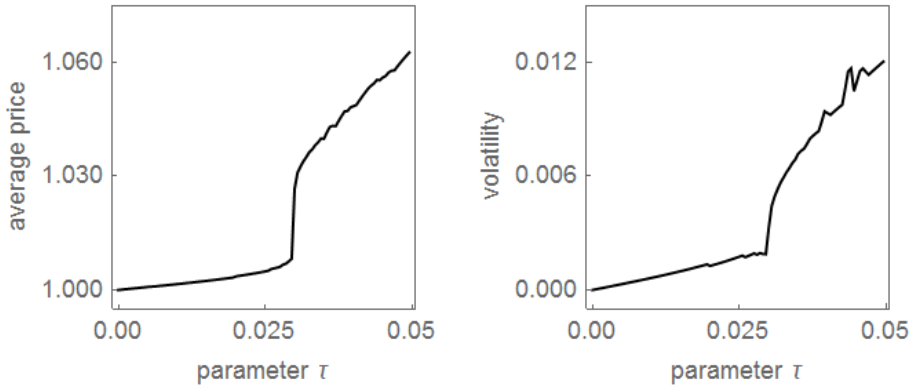

Figure 14: Average price and volatility as a function of parameter τ. The left (right) panel depicts the average price of the risky asset (the volatility of the risky asset) as a function of the tax rate. Parameter setting as in Figure 13, except that parameter τ is varied as indicated on the axis.

5 Conclusions

While policymakers around the world tax speculators' capital gains, as documented in Littlewood and Elliffe (2017), the equilibrium and out-of-equilibrium effects of capital gains taxes remain unclear, as revealed by the contrasting views offered by Klein (1999), Poterba and Weisbenner (2001), Ayers et al. (2003) and Dai et al. (2008). In this paper, we are particularly interested in the dynamic consequences of capital gains taxes. Based on a stylized behavioral asset-pricing model along the lines of Brock and Hommes (1998), we find that the imposition of capital gains taxes causes a natural nonlinearity, which, in turn, may give rise to endogenous asset price dynamics. The driving force behind such dynamics is rooted in the coexistence of two different regimes – one relevant in upward trending markets, when speculators expect to make capital gains and thus anticipate having to pay capital gains taxes, and the other relevant in downward trending markets, when they do not expect to make capital gains. Each of the two regimes is associated with a (different) fixed point. Since the stability properties of the fixed points depend on the underlying parameter setting, a number of interesting results emerge. Most importantly, we find that the imposition of capital gains taxes may create excess volatility and systematic mispricing, although the price of the risky asset would converge towards its fundamental value in the absence of capital gains taxes. Note that the empirical studies by Blouin et al. (2003), Jin (2006), George and Hwang (2007) and Jacob (2018) suggest that the imposition of capital gains taxes may inflate the prices of risky assets, too. For completeness, we mention that capital gains taxes may also, in principle, yield bounded dynamics, instead of otherwise divergent dynamics, although the parameter space that guarantees such outcomes seems to us to be quite limited. Finally, even if the price of the risky asset converged towards its fundamental value in the presence of capital gains taxes, tiny exogenous shocks could initiate significant (temporary) swings in the price of the risky asset.

Arguably, our conclusions with respect to the destabilizing nature of capital gains taxes rest on a stylized behavioral asset-pricing model. Due the simplicity of the model, however, we are able to derive a number of clear-cut analytical and numerical insights that may help us to better judge capital gains taxes. Despite the robustness checks we performed in our paper, more work is required in this exciting research direction – and we

hope that our study provides fresh stimulus for such endeavors. One avenue for future research could be to compare the effects of proportional versus progressive capital gains tax systems. Note also that speculators can only invest in one risky asset in our model. A multi-asset framework may be able to address this issue. Another avenue for future research could be to consider that speculators conduct year-end tax trading. Extending our model such that every period has two sub-periods – a "normal" mid-year period and a year-end period, where speculators consider their possible tax duties – may produce relevant insights. It might also be worth assuming that speculators must only pay capital gains taxes if their capital gains exceed a certain threshold. Relatedly, we consider only two possible regimes in our paper: a capital gains tax regime, relevant when speculators expect the price of the risky asset to increase, and a regime with no capital gains tax, relevant when speculators expect the price of the risky asset to decrease. An interesting model extension could be to consider a third possible regime, relevant when the price of the risky asset changes only moderately. Speculators' demand for the risky asset could then be represented as an average of the demand for the risky asset they would hold in the other two regimes. Moreover, one could consider that not all speculators switch simultaneously from one demand schedule to another because they expect a reversal of the risky asset market's direction, causing them to make capital gains taxes or not. For instance, their expectation rules could contain a random term that lends more heterogeneity to speculators' behavior. The goal of our paper is to point out a number of destabilizing forces associated with capital gains taxes – there may also be stabilizing forces attached to such a policy, which may emerge from alternative modeling setups.

References

Anufriev, M. and Hommes, C. (2012): Evolutionary selection of individual expectations and aggregate outcomes in asset pricing experiments. American Economic Journal: Microeconomics, 4, 35-64.

Anufriev, M. and Tuinstra, J. (2013): The impact of short-selling constraints on financial market stability in a heterogeneous agents model. Journal of Economic Dynamics and Control, 37, 1523-1543.

Avrutin, V., Gardini, L., Schanz, M., Sushko, I. and Tramontana, F. (2019): Continuous and discontinuous piecewise-smooth one-dimensional maps: invariant sets and bifurcation structures. World Scientific, Singapore.

Ayers, B., Lefanowicz, C. and Robinson, J. (2003): Shareholder taxes in acquisition premiums: the effect of capital gains taxation. Journal of Finance, 58, 2783-2801.

Beja, A. and Goldman, M. (1980): On the dynamic behaviour of prices in disequilibrium. Journal of Finance, 34, 235-247.
Blouin, J., Raedy, J. and Shackelford, D. (2003): Capital gains taxes and equity trading: empirical evidence. Journal of Accounting Research, 41, 611-651.
Brock, W. and Hommes, C. (1998): Heterogeneous beliefs and routes to chaos in a simple asset pricing model. Journal of Economic Dynamics and Control, 22, 1235-1274.
Chiarella, C., Dieci, R. and He, X.-Z. (2009): Heterogeneity, market mechanisms, and asset price dynamics. In: Hens, T. and Schenk-Hoppé, K.R. (eds.): Handbook of financial markets: dynamics and evolution. North-Holland, Amsterdam, 277-344.
Dai, Z., Maydew, E., Shackelford, D. and Zhang, H. (2008): Capital gains taxes and asset prices: capitalization or lock-in? Journal of Finance, 63, 709-742.
Day, R. and Huang, W. (1990): Bulls, bears and market sheep. Journal of Economic Behavior and Organization, 14, 299-329.
Dercole, F. and Radi, D. (2020): Does the "uptick rule" stabilize the stock market? Insights from adaptive rational equilibrium dynamics. Chaos, Solitons and Fractals, 130, 109426.
Dieci, R. and He, X.-Z. (2018): Heterogeneous agent models in finance. In: Hommes, C. and LeBaron, B. (eds.): Handbook of computational economics: heterogeneous agent modeling. North-Holland, Amsterdam, 257-328.
Gandolfo, G. (2009): Economic dynamics. Springer, Berlin.
George, T. and Hwang, C.-Y. (2007): Long-term reversals: overreaction or taxes? Journal of Finance, 62, 2865-2896.
Glaeser, E. (2013): A nation of gamblers: real estate speculation and American history. American Economic Review, 103, 1-42.
Glaeser, E. and Nathanson, C. (2017): An extrapolative model of house price dynamics. Journal of Financial Economics, 126, 147-170.
He, X.-Z., Li, Y. and Zheng, M. (2019): Heterogeneous agent models in financial markets: A nonlinear dynamics approach. International Review of Financial Analysis, 62,135-149.
Heemeijer, P., Hommes, C., Sonnemans, J. and Tuinstra, J. (2009): Price stability and volatility in markets with positive and negative expectations feedback: an experimental investigation. Journal of Economic Dynamics and Control, 32, 1052-1072.
Hirshleifer, D. (2001): Investor psychology and asset pricing. Journal of Finance, 56, 1533-1597.
Hommes, C., Sonnemans, J., Tuinstra, J. and van de Velden, H. (2005): Coordination of expectations in asset pricing experiments. Review of Financial Studies, 18, 955-980.
Hommes, C. (2013): Behavioral rationality and heterogeneous expectations in complex economic systems. Cambridge University Press, Cambridge.
Huang, W. and Day, R. (1993): Chaotically switching bear and bull markets: the derivation of stock price distributions from behavioral rules. In: Day, R. and Chen, P. (eds.): Nonlinear dynamics and evolutionary economics. Oxford University Press, Oxford, 169-182.
Huang, W., Zheng, H. and Chia, W.M. (2010): Financial crisis and interacting heterogeneous agents. Journal of Economic Dynamics and Control, 34, 1105-1122.
Huang, W. and Zheng, H. (2012): Financial crisis and regime-dependent dynamics. Journal of Economic Behavior and Organization, 82, 445-461.
Jacob, M. (2018): Tax regimes and capital gains realizations. European Accounting

Review, 27, 1-21.
Jin, L. (2006): Capital gains tax overhang and price pressure. Journal of Finance, 61, 1399-1431.
Klein, P. (1999): The capital gain lock-in effect and equilibrium returns. Journal of Public Economics, 71, 355-378.
Littlewood, M. and Elliffe, C. (2017): Capital gains taxation: a comparative analysis of key issues. Edward Elgar, Cheltenham.
Lux, T. (1995): Herd behaviour, bubbles and crashes. Economic Journal, 105, 881-896.
Martin, C., Schmitt, N. and Westerhoff, F. (2021): Heterogeneous expectations, housing bubbles and tax policy. Journal of Economic Behavior and Organization, 183, 555-573.
Medio, A. and Lines, M. (2001): Nonlinear dynamics: a primer. Cambridge University Press, Cambridge.
Milnor, J. (1985): On the concept of attractor. Communications in Mathematical Physics, 99, 177-195.
Poterba, J. and Weisbenner, S. (2001): Capital gains tax rules, tax-loss trading, and turn-of-the-year returns. Journal of Finance, 56, 353-368.
Puu, T. (2013): Attractors, bifurcations and chaos: nonlinear phenomena in economics. Springer, Berlin.
Simon, H. (1955): A behavioral model of rational choice. Quarterly Journal of Economics, 9, 99-118.
Tramontana, F., Westerhoff, F. and Gardini, L. (2010): On the complicated price dynamics of a simple one-dimensional discontinuous financial market model with heterogeneous interacting traders. Journal of Economic Behavior and Organization, 74, 187-205.
Tramontana, F., Westerhoff, F. and Gardini, L. (2013): The bull and bear market model of Huang and Day: Some extensions and new results. Journal of Economic Dynamics and Control, 37, 2351-2370.
Tversky, A. and Kahneman, D. (1974): Judgment under uncertainty: heuristics and biases. Science, 185, 1124-1131.
Westerhoff, F. (2008): The use of agent-based financial market models to test the effectiveness of regulatory policies. Jahrbücher für Nationalökonomie und Statistik, 228, 195-227.
Westerhoff, F. and Franke, R. (2018): Agent-based models for policy analysis: two illustrative examples. In: Chen, S.-H., Kaboudan, M. and Du, Y.-R. (eds.): The Oxford handbook of computational economics and finance. Oxford University Press, Oxford, 520-558.
Zeeman, E.C. (1974): On the unstable behaviour of stock exchanges. Journal of Mathematical Economics, 1, 39-49.